Macromolecules

ARTICLE

pubs.acs.org/Macromolecules

Miscibility of Poly(vinyl alcohol)-*graft*-Hydroxy Ester/ Poly(vinylpyrrolidone) Blends

Ainhoa Lejardi, Emilio Meaurio,* Jorge Fernández, and Jose-Ramon Sarasua*

School of Engineering, University of the Basque Country (EHU-UPV), Alameda de Urquijo s/n, 48013 Bilbao, Spain

ABSTRACT: Poly(vinyl alcohol) (PVA) grafted with different hydroxy acids (lactic acid (LA), glycolic acid (GA), and hydroxybutyric acid (HB)) has been blended with poly(vinylpyrrolidone) (PVP) and the miscibility of the *g*-PVA/PVP blends has been investigated by DSC, FTIR, and molecular modeling. Complete miscibility has been established by DSC for all the systems. The hydrogen-bonded (HB) C═O stretching band of PVP shows a larger red shift than in other polyol/PVP systems. In addition, *g*-PVA rich blends show a second, highly red-shifted, contribution assigned to double hydrogen bonds. Since this feature is very unusual in polymer blends, the strength of the interactions has been investigated using *ab initio* QM methods. The interaction energies have been calculated in model compounds for PVA and the polymeric blends at the MP2/cc-pVTZ//MP2/cc-pVDZ level of theory. The infrared spectra of different model compounds and their complexes have also been analyzed. According to the QM analysis, the C═O groups in the pyrrolidone ring and the C═O groups in the hydroxy ester residues adopt antiparallel arrangements establishing attractive dipole−dipole interactions. The analysis of the models suggests that the intermolecular interaction between the hydroxy ester residues in *g*-PVA and the C═O groups in PVP is stronger than the autoassociation of PVA or *g*-PVA, providing energetic arguments to explain the occurrence of double HB-s in the condensed phases. The model compounds provide information about the relative strength of the interactions in the polymeric systems.

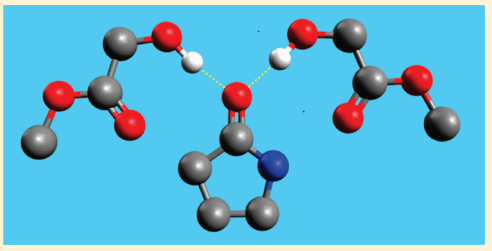

INTRODUCTION

In recent years, the miscibility of different polymers has been studied to obtain new materials exhibiting different properties from those of the existing homopolymers or copolymers.[1] The miscibility of two different polymers is enhanced by exothermic intermolecular interactions such as ion−ion, dipole−dipole, ion−dipole, and hydrogen-bonding interactions. These interactions are considered to play a key role in polymer compatibility, eventually resulting in homogeneous materials with continuous physical properties. From a thermodynamic point of view, a negative free energy of mixing (ΔG_m) is necessary to achieve the miscibility of polymer pairs.[2]

Poly(vinyl alcohol) (PVA) is a well-known water-soluble polymer with high transparency and outstanding mechanical and thermal properties. Therefore, PVA has been widely used in textiles, paints, building materials, electronic products, automotive, aerospace, medicine, paper making, printing, packaging, and other industries.[2] It is often used blended with other polymers to improve the properties of the bulk material or solution. Certain polymers such as cellulose (and its derivatives) and poly(vinylpyrorrolidone) (PVP) are known to be miscible with PVA, presumably due to hydrogen-bonding interactions between the hydroxyl groups of PVA and appropriate interacting sites in the blend partner (carbonyl groups of PVP and secondary hydroxyl groups of cellulose).[3−6] PVP is an amorphous polymer of high environmental stability, easy processability, and moderate thermal conductivitity.[3] It is also one of the most commonly used polymers in medicine because of its solubility in water and its extremely low cytotoxicity.[6] PVP also possesses a marked Lewis basic character, and its carbonyl group located in the side pyrrolidone ring is prone to the formation of intermolecular hydrogen bonds with the proton-donating polymers (Lewis acids).[8]

Our research group is investigating the chemical modification of PVA as a route to improve its compatibility/miscibility with selected immiscible counterparts. Particularly, grafting the PVA chain with hydroxy acids (HA) replaces the hydroxyl groups of the PVA chain by lateral hydroxyalkyl ester groups. The larger volume of the new lateral groups results in the reduction of the density of hydroxyl groups in the final polymer, therefore reducing the autoassociation density and consequently its solubility parameter. Since miscibility is favored with the reduction of the difference in solubility parameters between the blend partners, decreasing the large solubility parameter of PVA should favor its miscibility with most of the polymer partners of interest, which typically present much smaller solubility parameters. In addition, the grafted copolymers are completely amorphous, and their physical and mechanical properties are completely different from those of PVA. Since they are constructed exclusively from biodegradable building blocks, biodegradability and biocompatibility can be also expected (their biodegradability is not, however, investigated here). Hence, their blends with appropriate counterparts such as PVP could find application in the biomedical field, aside from those of the pure materials. Therefore, the aim of this work is to study the miscibility between the graft copolymers of PVA and poly(vinylpyrrolidone). Even though PVA forms miscible

Received: May 31, 2011
Revised: August 12, 2011
Published: September 02, 2011

ACS Publications © 2011 American Chemical Society

Scheme 1. Esterification of PVA with DL-Lactic Acid

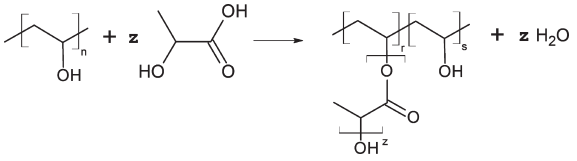

Table 1. Reaction Feed Ratios, Compositions, Naming Conventions, Degree of Polymerization of the Grafted Chain (See Scheme *1*), and Glass Transitions for the Polymers Synthesized in This Study

hydroxy acid	molar feed ratio [HA]/[PVA]	grafted HA (mol %)	copolymer name	deg of polym, z	T_g (°C)
			PVA		74
LA	1/1	28	VALA28	1.1	57
LA	4/1	45	VALA45	1.1	68
GA	1/4	24	VAGA24	1.1	38
GA	4/1	44	VAGA44	1.3	48
HB	4/1	14	VAHB14	1.1	60

blends with PVP, the grafting reaction introduces up to nearly 50 mol % of hydroxy acid groups that should exert a profound influence in the miscibility behavior of the blends.

MATERIALS AND METHODS

Materials. Poly(vinylpyrrolidone), PVP (M_w 360 000), was obtained from sigma Aldrich. PVA was esterified with varying feed ratios of racemic lactic acid (LA), glycolic acid (GA), and racemic hydroxybutyric acid (HB) to obtain modified polymers of different composition (see Scheme 1). Reaction conditions can be found elsewhere.[9]

Nuclear Magnetic Resonance (NMR). ^{1}H and ^{13}C NMR spectra were recorded in a Bruker Avance DPX 300, which corresponds to 300.16 and 75.5 MHz frequencies for ^{1}H and ^{13}C, respectively, in 5 mm o.d. sample tubes using 0.7 mL of deuterated dimethyl sulfoxide (DMSO-d_6) at room temperature (≈30 °C). The analysis of the ^{1}H and ^{13}C NMR spectra (details can be found in ref9; Table 1 contains the relevant results) indicates random grafting, with hydroxyacid compositions in the range 14−45 mol % and degrees of polymerization (z, see also Scheme 1) close to unity.

Preparation of Blends. Polymer blends were prepared by solvent casting using water as solvent. Solutions were then cast onto glass plates, and the solvent was evaporated a under vacuum at 50 °C for a week.

Thermal Analysis. Thermal analysis was carried out on a differential scanning calorimeter (DSC) from TA Instruments, model DSC 2920. Aluminum pans containing 5−10 mg of sample were used in all cases. Two consecutive scans were performed with a scan rate of 20 °C min^{-1}, up to 200 °C, under a nitrogen atmosphere. Glass transition temperatures were obtained in the second scan and were measured as middle point values.

Infrared Spectroscopy (FTIR). Infrared spectra were recorded on a Nicolet AVATAR 370 Fourier transform infrared spectrophotometer (FTIR). Samples were prepared by casting 0.2 wt % hexafluoroisopropanol (HFIP) solutions on KBr pellets.

Computational Methods. *Ab initio* QM calculations have been performed on several model compounds and their complexes. Generated structures were first optimized using the MMFF94s force field implemented in Avogadro, then optimized using the PM3 semiempirical method, and finally optimized using the second-order Møller−Plesset perturbation theory. In case of single molecules, electronic energies were calculated at the MP2/cc-pVQZ//MP2/cc-pVTZ level of theory (the notation indicates that single point MP2/cc-pVQZ energies were calculated using the geometries optimized at the MP2/cc-pVTZ level). Similarly, the electronic energies of the complexes and clusters were calculated at the MP2/cc-pVTZ//MP2/cc-pVDZ level. Every geometry (excluding clusters with $N \geq 4$) was confirmed to be a local minimum by calculating the vibrational frequencies at the MP2/cc-pVDZ level of theory. Basis set superposition error (BSSE) has been accounted for by doing the Boys and Bernardi counterpoise (CP) correction.[10] The CP corrected total energy for the AB complex, E(AB), and the CP corrected interaction energy, E_{int}(AB), were calculated according to

$$E(\mathrm{AB}) = E_{\mathrm{AB}}^{\mathrm{AB}} + (E_{\mathrm{A}}^{\mathrm{A}} - E_{\mathrm{A}}^{\mathrm{AB}}) + (E_{\mathrm{B}}^{\mathrm{B}} - E_{\mathrm{B}}^{\mathrm{AB}}) \quad (1)$$

$$E_{\mathrm{int}}(\mathrm{AB}) = E_{\mathrm{AB}}^{\mathrm{AB}} - E_{\mathrm{A}}^{\mathrm{AB}} - E_{\mathrm{B}}^{\mathrm{AB}} \quad (2)$$

where the subscripts refer to the system (adopting the same geometry as in the optimized complex) and the superscripts refer to the basis set. The *ab initio* calculations were performed using the Firefly QC package,[11] which is partially based on the GAMESS (US)[12] source code. MacMolPlt 7.4.2 was used for the analysis of results.[13]

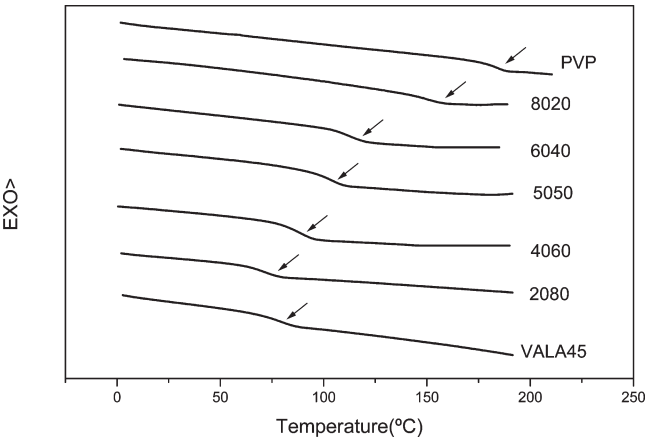

Figure 1. Second scan DSC traces for VALA45, PVP, and VALA45/PVP blends of different composition (w/w).

RESULTS AND DISCUSSION

Miscibility Analysis. The criterion most commonly used to ascertain the miscibility of two polymers is the existence of a single glass-transition temperature for the blend located between the glass-transition temperatures of the pure polymers.[14,15] Since the glass transition temperature of PVP occurs at 178 °C, about 130 °C above the T_gs of the grafted copolymers (see Table 1), DSC is appropriate for the analysis of the miscibility in these systems. Figure 1 shows the second scan DSC traces for the VALA45/PVP system. As can be seen, a single glass transition temperature, intermediate to those of the pure components, can be observed regardless of the composition. Similar results have been observed for the blends prepared with the remaining graft copolymers investigated in this work and PVP. Therefore, DSC results indicate miscibility for all the graft copolymers with PVP in the whole range of compositions.

Figure 2 illustrates the dependence of T_g on composition for some of the blends analyzed in this work. Assuming the additivity of the specific volumes, (indeed equivalent to assuming the additivity of free volumes), Gordon and Taylor[16] derived the

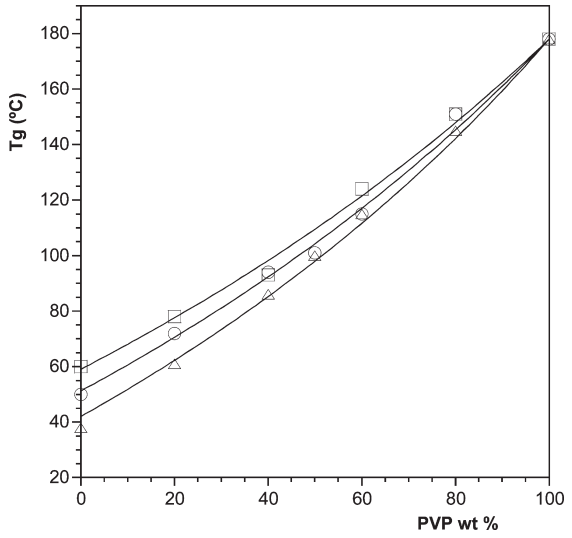

Figure 2. T_g vs composition for different *g*-PVA/PVP blends: (□) VAHB14/PVP, (○) VALA45/PVP, and (△) VAGA24/PVP. The continuous line is obtained fitting the experimental points to the Fox equation.

following equation for the dependence of T_g on composition:

$$T_g = \frac{w_1 T_{g1} + K w_2 T_{g2}}{w_1 + K w_2} \quad (3)$$

where T_g is the glass transition temperature of the blend, w_i are the weight fractions of the components, T_{gi} represent the glass transition temperatures of the blend components, and $K = (\rho_1/\rho_2)(\Delta\alpha_2/\Delta\alpha_1)$. In the latter expression, ρ_i are the densities and $\Delta\alpha_i = (\alpha_{melt} - \alpha_{glass})$ the increments at the T_g of the expansion coefficients of the blend components. Values of $\Delta\alpha_i$ can be estimated assuming the validity of the Simha−Boyer rule, $\Delta\alpha T_g = 0.133$ (constant).[17] In addition, if the difference in density between the blend components is also neglected, $\rho_1/\rho_2 \approx 1$, the Gordon−Taylor equation simplifies to the well-known Fox equation:[18]

$$\frac{1}{T_g} = \frac{w_1}{T_{g1}} + \frac{w_2}{T_{g2}} \quad (4)$$

These equations were initially derived for random copolymers and then subsequently extended without further modifications to miscible polymer blends. As can be seen in Figure 2, the dependence of T_g on composition for the systems investigated in this paper shows the typical concave curvature of systems obeying the Fox equation, suggesting "ideality" in the sense the observed behavior suggests the additivity of the free volumes in the blends.

FTIR Analysis. FTIR spectroscopy is particularly sensitive to specific interactions and has been widely used in the detection and analysis of the strength of hydrogen-bonding contacts. Polymer miscibility is usually driven by specific interactions, which usually lead to band shifting/broadening in the blends, compared to the infrared spectra of the pure homopolymers.[19] Figure 3 shows the hydroxyl stretching region (3500−3000 cm^{-1}) for the VAGA44/PVP system (upper part). The spectra for the PVA/PVP system are also shown for comparison purposes (bottom part). In polymers containing hydroxyl groups, the OH moieties can be "free", but most of them tend to be associated in the form of dimers

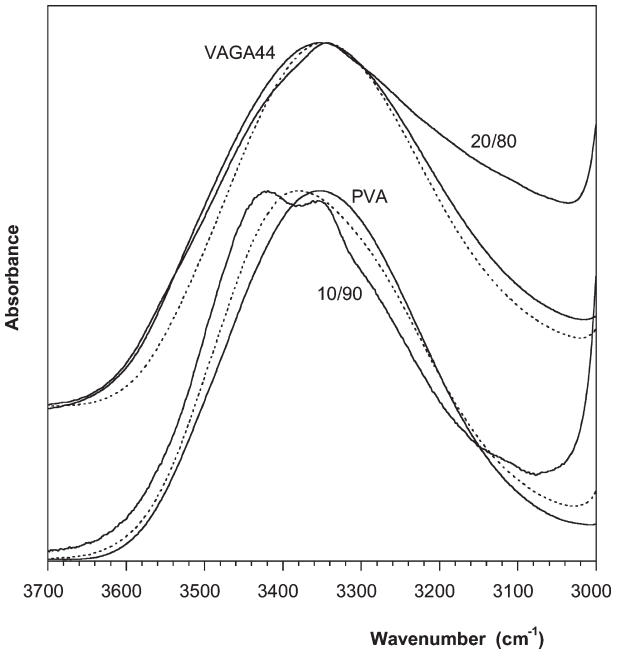

Figure 3. Hydroxyl stretching region for PVA/PVP blends (bottom part) and for VAGA44/PVP blends (upper part). Dotted line spectra correspond to the 60/40 composition.

and multimers.[20] There is a wide range of species and geometries and therefore of hydrogen bonding strengths, and the hydroxyl stretching region can be considered a continuous band composed of very closely spaced contributions. Hence, both PVA and VAGA44 show broad bands centered at about 3350 cm^{-1}, reflecting a wide range of interactions. Compared to neat PVA, the hydroxyl stretching band of pure VAGA44 is broader and is slightly shifted to higher wavenumbers (about 5 cm^{-1}), a result that can be accounted for considering that hydroxyl−ester interactions should also occur in this system.

In the PVA/PVP system blending shifts the hydroxyl stretching band to higher wavenumbers up to about 3420 cm^{-1} for the 10/90 composition. The absorption corresponding to hydroxyl−carbonyl interactions can be assumed to occur at this location, since at this composition the interassociation of hydroxyl groups is favored over autoassociation due to the large excess of acceptor groups.[6] The frequency difference ($\Delta\nu$) between the hydrogen-bonded hydroxyl absorption and the free hydroxyl absorption is known to provide a measure of the average strength of the intermolecular interaction;[21,22] hence, hydroxyl−hydroxyl autoassociation is stronger than hydroxyl−ester interassociation in the PVA/PVP system. The "free" OH band of PVA is known to occur at about 3615 cm^{-1};[23,24] therefore, the red shift corresponding to the intermolecular interactions in the PVA/PVP system is $\Delta\nu = 195$ cm^{-1}.

On the contrary, blending VAGA44 with PVP slightly shifts the hydroxyl stretching band to lower wavenumbers, up to about 3345 cm^{-1} for the 20/80 composition. The same behavior is observed in the VAGA24/PVP, VALA28/PVP, and VALA45/PVP systems. The main contribution observed for the PVP-rich compositions, again attributable to the intermolecular interactions, occurs at a clearly different location from that observed in the PVA/PVP system, indicating that it arises from different interactions. Hence, the contribution at about 3345 cm^{-1} is attributed to hydrogen-bonding interactions between the terminal hydroxyl

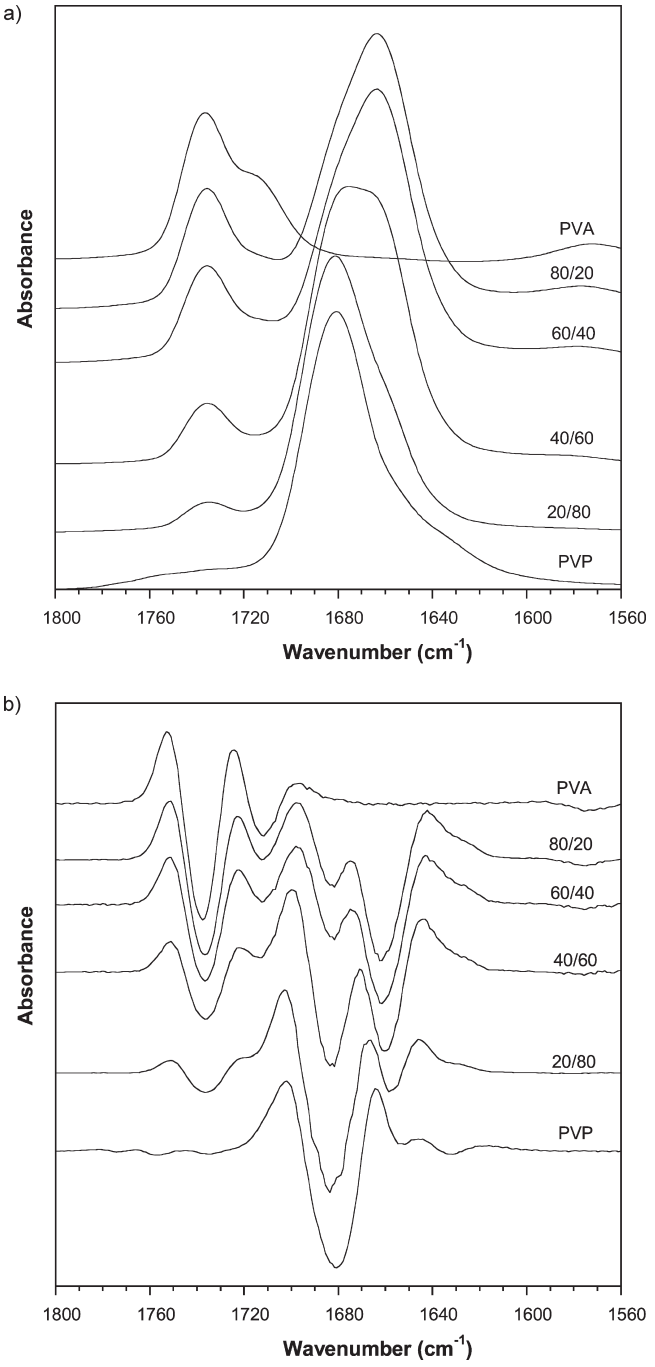

Figure 4. (a) Carbonyl stretching region for PVA/PVP blends. (b) Second-derivative spectra of the carbonyl stretching region for the PVA/PVP blends.

groups located in the lateral hydroxyester chains and the carbonyl groups in PVP. Notice that even though in these copolymers the amount of hydroxyl groups located in vinyl alcohol segments exceeds the amount of OH groups located in the lateral hydroxy ester chains, interassociation occurs preferentially with the latter. Assuming that the "free" hydroxyl groups also absorb at 3615 cm^{-1}, the new shift $\Delta\nu$ = 270 cm^{-1} indicates interassociation interactions of larger average strength in the new systems. Assuming a Rozenberg type relationship[22] between the hydrogen-bonding strength and the frequency shift ($\Delta H \propto (\Delta\nu)^{1/2}$), the hydrogen-bonding interactions in the grafted systems are ~20% stronger than in the PVA/PVP system.

In the *g*-PVA/PVP system, the nearly constant shape of the hydroxyl stretching band upon addition of PVP indicates that the strength of the new O—H···O=C interactions is similar to that of the OH···OH interactions they replace to. This behavior agrees with the dependence on composition observed for the T_g of the system, since free volume additivity is to be expected when the strength of the interactions does not change noticeably upon blending.[15] Finally, the VAHB14/PVP system shows an intermediate behavior between the two scenarios discussed in Figure 3. In this system, adding PVP to the copolymer shifts the hydroxyl band to higher wavenumbers up to about 3385 cm^{-1} in the case of the 20/80 composition. The difference in behavior could be partly attributed to the low degree of substitution in this system, but other possible factors will be discussed later in this paper.

Figure 4 displays the C=O stretching band for the poly(vinyl alcohol)/poly(vinylpyrrolidone) (PVA/PVP) blends. This system is characterized first to discern its hydrogen-bonding interactions from those involving the hydroxyl groups located in the grafted residues in the *g*-PVA/PVP system. The PVA sample blended with PVP in Figure 4 is actually a "Mowiol" commercial grade containing about 12% of residual acetate units distributed in blocky sequences as a consequence of the saponification reaction.[25] The second-derivative spectrum of pure Mowiol shows two bands in the C=O stretching region: the component at about 1737 cm^{-1} is attributed to "free" C=O groups in the vinyl acetate segments and the band at about 1712 cm^{-1} to hydrogen-bonded C=O groups. As can be seen, the "free" contribution dominates the C=O stretching region of pure Mowiol, and the relative intensity of these two bands remains unaffected by blending. The larger intensity of the "free" band can be attributed to the segregation of the blocky vinyl acetate segments to a second phase (recall that poly(vinyl acetate) is immiscible with poly(vinyl alcohol)).[26]

The C=O stretching band of pure PVP is located at about 1682 cm^{-1} (Figure 4) and its large width (half-height width 35 cm^{-1}) is attributed to the occurrence of a broad range of interactions in the pure polymer.[27−29] In addition to band broadening, the C=O stretching band is known to shift to lower wavenumbers due to the dipole−dipole interactions.[27−30] Hence, the spectrum of the pure polymer does not reflect the actual width and location corresponding to the stretching mode of the truly "free" C=O groups. For example, the C=O stretching band of liquid acetone is red-shifted by about 19 cm^{-1} compared to the gas phase, and most of this bathochromic shift is attributed to the dipole−dipole interactions occurring in the condensed phase.[30] In case of PVP, dilution of the vinylpyrrolidone segments is known to decrease the width of the C=O stretching band from 35 cm^{-1} to up to about 10 cm^{-1}.[27,28] However, the actual location of the truly free vinylpyrrolidone segments can be hardly established since the diluting agent also affects the location of the C=O stretching band.[30]

In blends of PVP with PVA a new component can be observed at about 1660 cm^{-1}, attributed to C=O groups of PVP hydrogen bonded with the hydroxyl groups of PVA.[6] The same location was also observed for the HB contribution in blends of PVP with poly(vinylphenol) (PVPh).[31] Considering the discussion about the behavior of the C=O stretching band of pure PVP, the observed shift, 22 cm^{-1}, measures the shift relative to C=O stretching band in pure PVP, rather than with the actually "free" C=O groups.

As can be seen in Figures 5a and 5b, blending of PVP with VAGA44 results in complex carbonyl bands, with unusual

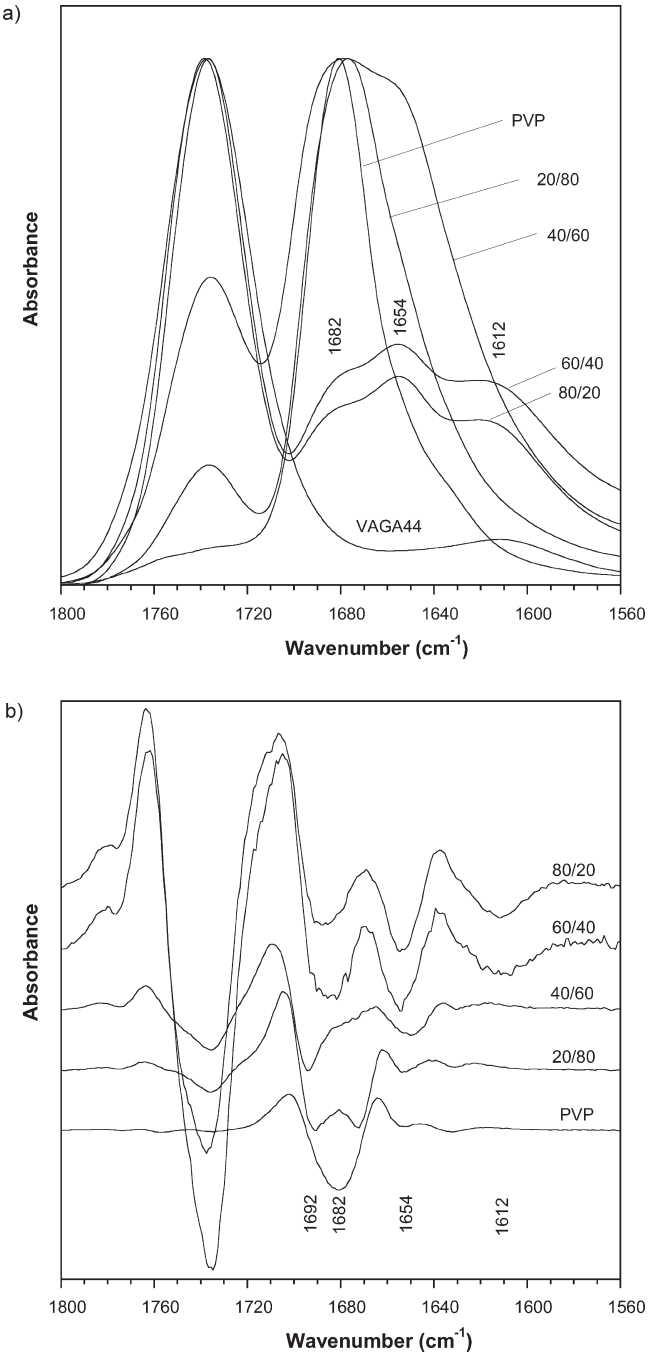

Figure 5. (a) Carbonyl stretching region for VAGA44/PVP blends. (b) Second-derivative spectra of the carbonyl stretching region for the VAGA44/PVP blends.

spectral features compared to typical systems containing hydroxyl−carbonyl hydrogen bonds. The PVP-rich blends (VAGA44/PVP 20/80 and 40/60 compositions) show a narrow (see second derivative) component blue-shifted by about 10 cm^{-1} relative to pure PVP. Since this component occurs in PVP-rich systems, it can be hardly attributed exclusively to a dilution effect, and the molecular modeling results (next section in this paper) suggest that it might arise from specific repulsive dipole−dipole interactions. Actually, the new narrow component seems overlapped with the absorption band corresponding to regular C═O groups in PVP (see the second derivative corresponding to the 40/60 composition in Figure 5b).

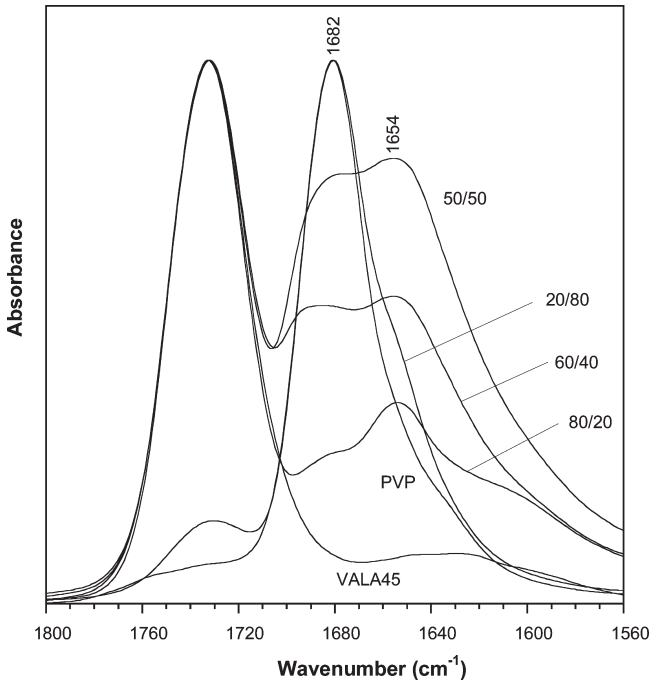

Figure 6. Carbonyl stretching region for VALA45/PVP blends.

In addition, a new component located at about 1654 cm^{-1} can be observed for all the compositions. Compared to the location observed in the PVA/PVP system, this band is additionally red-shifted by about 6 cm^{-1}, suggesting that it should be attributed to carbonyl groups of PVP hydrogen bonded with the hydroxyl groups located in the grafted residues of the copolymer rather than with the hydroxyl groups of the vinyl alcohol segments. Finally, in blends containing an excess of the graft copolymer (VAGA45/PVP 60/40 and 80/20 compositions), a new component can be observed at about 1612 cm^{-1}, red-shifted by about 70 cm^{-1} relative to the location of pure PVP.

The lower wavenumber component could be attributed to double hydrogen bonds in which the C═O group acts as acceptor and two hydroxyl groups act as donors. However, this type of hydrogen-bonding interaction is very unusual in polymers in the solid state; they have been found to occur between polymers and small molecules in solution,[33] but not between macromolecules in a high-viscosity environment. An alternative explanation is to consider that the second donor molecule is actually residual monomer (glycolic acid in case of the VAGA44/PVP system). However, the amount of residual monomer necessary to explain the band at 1612 cm^{-1} is unreasonably large. The grafted copolymers were carefully purified, including Soxhlet extraction with acetone for 24 h, and the analysis of the ^{1}H and ^{13}C NMR spectra excludes the presence of large amounts of residual monomer.[9] Therefore, the band at 1612 cm^{-1} is definitely assigned to double hydrogen bonds, a conclusion additionally supported by the molecular modeling analyses included in the following section.

Finally, Figure 6 displays the C═O stretching region for the VALA45/PVP system. In general, the spectra are rather similar to those discussed for the VAGA44/PVP system. Again, the O−H···O═C hydrogen-bonding band occurs at about 1654 cm^{-1}. For the 60/40 and 80/20 compositions the lower wavenumber component located at about 1612 cm^{-1} can be also observed, but in this system its relative intensity is smaller at a fixed composition. This difference

dx.doi.org/10.1021/ma2012305 |*Macromolecules* 2011, 44, 7351–7363

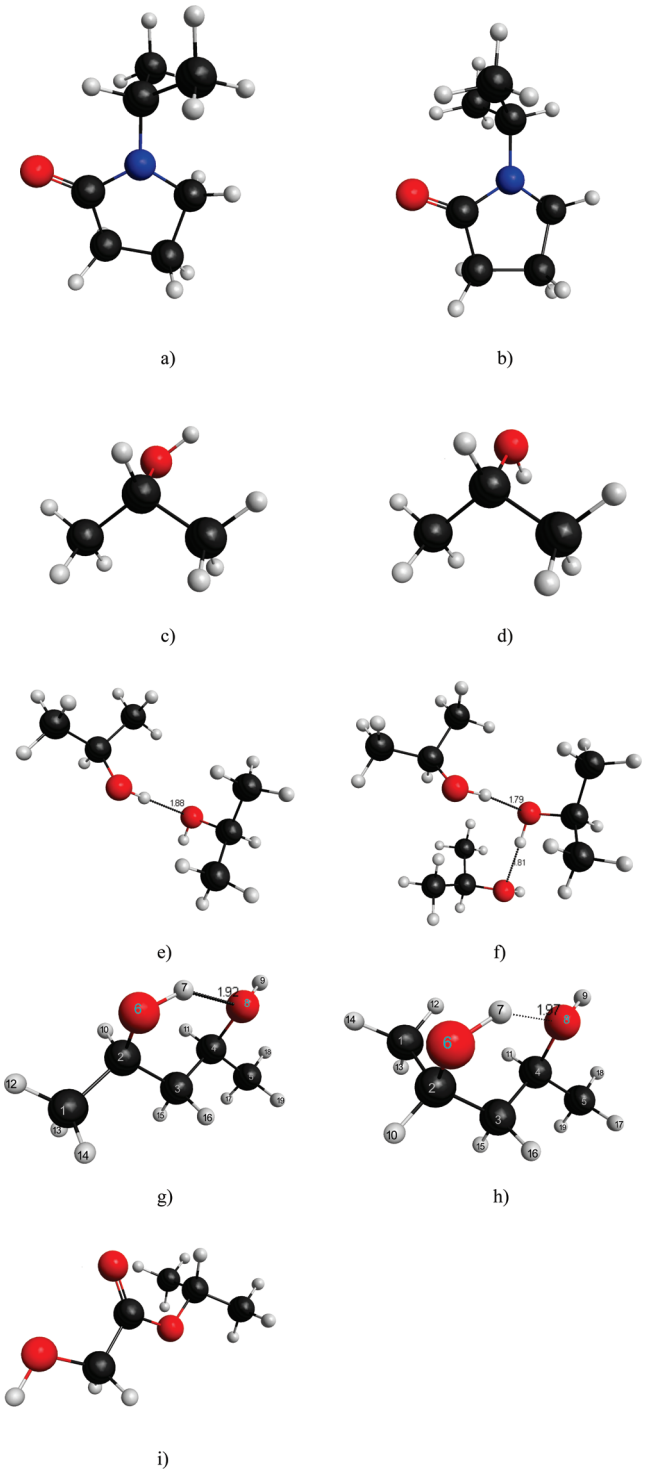

Figure 7. Equilibrium conformers for (a, b) 2-pyrrolidonylpropane (PP), (c, d) 2-hydroxypropane (HP), (e, f) dimer and trimer of HP (constructed using **7c** conformers), (g) 2*R*,4*S*-dihydroxypentane (m-DHP), (h) 2*S*,4*S* dihydroxypentane (r-DHP), and (i) 2-glycolylpropane (GP). Geometries of single molecules at the MP2/cc-pVTZ level; HP clusters at the MP2/cc-pVDZ level.

will be also addressed in the following section dealing with the molecular modeling analysis of the systems.

Molecular Modeling. The aim of the following *ab initio* QM calculations is to gain insight into the nature and the strength of the apparently strong intermolecular interactions occurring in the g-PVA/PVP blends (compared to those of the PVA/PVP system) and eventually understand the observed spectral features. In this section, the stable geometries and the IR spectra of the selected model compounds and their complexes will be calculated and discussed. Even though calculations are carried out in the gas phase, the structures calculated for the most stable complexes should be also favored in the condensed phases, specially in systems with strong intermolecular interactions. For example, in liquid acetone it has been shown that the C═O bond dipole moment vectors of nearest neighbors tend to be oriented in antiparallel manner,[30,34] and this is actually the most stable structure obtained by QM calculations for an acetone dimer in the vapor phase.

In the PVP chain, the pyrrolidone side groups adopt two stable conformations which result in an eclipsed arrangement of the N−CH_2 or N−(C═O) and the C_α−H_α bonds,[35] but their relative stability is actually unknown. The model compound 2-pyrrolidonylpropane (PP) is adopted here to analyze the orientation of the pyrrolidone ring in PVP (see Figure 7). Only the C_α−N bond can be rotated in PP, and Figure 7 shows the geometries of the two stable conformers optimized at the MP2/cc-pVTZ level of theory. Conformer **7a** presents lower electronic energy and is stabilized through attractive 1,5 C_α−H_α···O═C interactions.[36,37]

Single-point electronic energies calculated at the MP2/cc-pVQZ//MP2/cc-pVTZ level for the conformers of PP have been corrected using the thermochemistry data calculated at the MP2/cc-pVTZ level according to the usual rigid rotor and harmonic normal mode approximations to obtain the ideal gas Gibbs free energies at 1 atm. The relative weight of each conformer in the gas-phase equilibrium has been obtained from the Boltzmann distribution based on the Gibbs energy, and the results are listed in Table 2. As can be seen in Table 2, conformer **7a** dominates the gas phase population of PP. Assuming that in condensed phases the pyrrolidone ring also adopts preferentially the orientation with eclipsed C═O and C_α−H_α bonds, only conformer **7a** of PP will be considered in the molecular models investigated in this paper.

PVA contains secondary hydroxyl groups, and the simplest molecular model containing these moieties is 2-hydroxypropane (HP). As can be seen in Figure 7, HP exists in three conformations: *trans*, *gauche*, and *gauche*-mirror.[38] In the trans rotamer (**7d**) the H atoms of the H−O−C2−H moiety are strictly in the trans orientation (C_s symmetry), and in the *gauche* and *gauche*-mirror the H atoms adopt skewed cisoid configurations (C_1).[38] In this paper, the geometry denoted **7c** in Figure 7 represents the two mirror conformers (not only the one actually shown). The Gibbs free energies of the trans and gauche conformers have been

Table 2. Selected Modeling Results for the Conformers of PP and HP[a]

conformer	$\Delta E^{MP2}_{cc\text{-}pVQZ//cc\text{-}pVTZ}$	ΔE_0	ΔH	$T\Delta S$	ΔG	pop (%)
7a	0	0	0	0	0	97
7b	5.4	5.5	5.2	−2.9	8.3	3
7c	0	0	0	0	0	78
7d	1.5	1.5	1.5	0	3.2	22

[a] Electronic energies, total energies at 0 K, thermochemistry data in the ideal gas phase at 298.15 K, and 1 atm and resulting equilibrium populations (see text).

Table 3. Number of Basis Functions, Interaction Energies (E_{in}), Interaction Energies Corrected for Deformation (E'_{in}), and BSSE Values Obtained at Different Levels of Theory for the Dimer of HP (7e)

theory level	$N_{basis\ func}$	E_{in} (kJ/mol)	E'_{in} (kJ/mol)	BSSE (kJ/mol)
cc-pVDZ	200	−18.1	−16.9	29.7
aug-cc-pVDZ//cc-pVDZ	344	−25.4	−24.5	12.4
cc-pVTZ//cc-pVDZ	520	−26.0	−24.6	12.1
cc-pVTZ	520	−26.3	−25.5	11.4
aug-cc-pVTZ//cc-pVTZ	840	−28.9	−28.4	5.5
cc-pVQZ//cc-pVTZ	1120	−29.1	−28.2	4.4
aug-cc-pVQZ//cc-pVTZ	1720	−30.0	−29.2	2.5

calculated following the same procedure used for PP, and after accounting for the degeneracy, the gauche conformer is predicted to prevail in the gas phase (see Table 3). This result agrees both with reported calculations and with the investigation of the Ar-matrix IR spectra of HP.[38] Therefore, the **7c** conformer of HP will be adopted in this paper to model the interactions in both pure PVA and its blends. Nevertheless, considering the relatively small difference of energy between conformers **7c** and **7d**, QM calculations have also been performed using the latter geometry. Since both geometries lead to similar results, only the analyses performed with the most stable conformer will be included here to simplify the discussion.

Figure 7e shows one equilibrium dimer of HP (built using conformer **7c**). Let us use this simple system to briefly analyze the accuracy of the ab initio methods used throughout this paper. Table 3 presents the number of basis functions, the interaction energies (E_{in}, eq 2), the interaction energies corrected for deformation (E'_{in}),[39] and the BSSE values calculated for the **7e** dimer at different levels of theory. The interaction energies corrected for deformation, E'_{in}, have been obtained adding to the "pure" interaction energies (eq 2) the deformation energies for the individual molecules participating in the dimer.[39] The deformation energy is usually a small unfavorable contribution, as reflected by the difference between the E_{in} and the E'_{in} values in Table 3. The most accurate interaction energy should be obtained from the largest basis sets and should account for deformation; hence, the "reference" interaction energy is about −29 kJ/mol. As can be seen in Table 3, the smaller basis sets tend to underestimate the interaction energy, and the small cc-pVDZ is clearly unappropriate. At least the aug-cc-pVDZ or the cc-pVTZ basis sets are necessary to obtain energies with acceptable accuracy, and the latter leads to slightly better results and is accepted to provide both reliable geometries and energies.[40−43] In addition, the geometries of the HP dimer optimized using the cc-pVDZ and the cc-pVTZ basis sets are very similar, as indicated by the similar energies obtained for the cc-pVTZ//cc-pVDZ and the cc-pVTZ calculations. Hence, considering both accuracy and computational efficiency, the MP2/cc-pVTZ//MP2/cc-pVDZ level of theory is chosen in this paper to obtain the total electronic energies and the interaction energies according to eqs 1 and 2. Finally, the BSSE shows the expected decrease as the size of the basis set increases, becoming small for the largest basis set.

However, the dimer of HP does not reflect the strength of the interactions in bulk HP. The energetics of alcohols in the condensed phase are known to depend on the hydrogen-bonding structure and on cooperativity.[44−47] The type of hydrogen-bonding

Table 4. Total Interaction Energies, E_{in}, Incremental Interaction Energies, ΔE_{in}, and Average Interaction Energies for Clusters of 2-Hydroxypropanol (HP) of Different Size

N	E_{in} (kJ/mol)	ΔE_{in} (kJ/mol)	$\hat{E}_{in}$ (kJ/mol)
2	−26.0		
3	−63.3	−37.3	−31.7
4	−101.7	−38.3	−33.9
5	−141.0	−39.3	−35.2
6	−180.5	−39.5	−36.1
7	−222.8	−42.3	−37.1

structures has been a controversial issue for years[44] but has been enlightened in recent papers in which autoassociation is proven to occur predominantly in the form of open chains.[44−46] The cyclic species, known to prevail in the gas phase because of their larger stabilities,[44] are only present in minor amounts in the condensed phases according to molecular dynamics (MD) analyses.[46] Cooperativity denotes the effect by which once a molecule engages as a HB donor; it automatically becomes a better acceptor and vice versa due to the polarization of the O−H bond.[47] Cooperative effects are usually examined considering trimolecular complexes,[48] and Figure 7f shows the simplest open complex containing three HP molecules (in **7c** conformation). The CP-corrected total interaction energies, E_{in} (also called binding energies), have been calculated according to

$$E_{in} = E^{clust}_{N\text{-mer}} - \sum_{i=1}^{N} E^{clust}_{i} \quad (5)$$

where $E^{clust}_{N\text{-mer}}$ is the total electronic energy calculated for the whole N-mer, and the E^{clust}_{i} terms represent the electronic energies for the individual i molecules calculated in the basis set of the cluster. Since cooperative effects can depend on chain length, we have investigated HP clusters containing up to 7 molecules, and Table 4 lists the calculated interaction energies and the incremental interaction energies, $\Delta E_{in} = E_{in,N} - E_{in,(N-1)}$. As can be seen, the interaction energy corresponding to the formation of a dimer is −26 kJ/mol, but the incremental interaction energy corresponding to the addition of the third HP unit amounts −37 kJ/mol, reflecting the cooperative strengthening. Notice that the increase of interaction energy observed upon the addition of the third molecule is not actually located in the new intermolecular contact; instead, the new interaction enhances the polarization of the central OH bond which becomes now both a stronger donor and acceptor.

As can be seen in Table 4, the values of ΔE_{in} increase slightly with the number of molecules in the cluster. This might reflect certain dependence of the cooperative strengthening with chain length, but additional factors might contribute to this behavior. Particularly, the addition of new molecules implies weak attractive VDW interactions between nonvicinal molecules, contributing to the total interaction energy, and therefore to ΔE_{in}. These effects can be accounted for through the calculation of the cooperative energy (E_{coop}).[48] The relatively small variation observed for ΔE_{in} suggests that cooperative strengthening becomes saturated very fast (perhaps with $N = 3$) and that its dependence with chain length is (if any) small. This result agrees with the fact that theoretical models dealing with cooperativity effects usually consider only two association constants, K_2, for the formation of dimers, and K_B, for the formation of multimers.[19]

Table 5. Dihedral Angles, Electronic Energies, and Hydrogen-Bonding Distances for the Most Stable HB and Non-HB Conformations of m-DHP and r-DHP

		dihedral angle (deg)[a]					
model comp	conf ID	φ_1	φ_2	ω_1	ω_2	ΔE^b (kJ/mol)	$d_{O\cdots H}$ (Å)
m-DHP	m1 (7 g)	169	−178	−76	−59	0.0	1.92
	m2	175	−175	−74	−174	1.2	1.95
	m3	56	175	59	−66	11.6	
	m4	60	176	−60	−65	11.7	
	m5	59	177	62	−179	13.0	
	m6	−58	−159	71	−63	14.5	
	m7	60	176	179	−179	14.8	
r-DHP	r1 (7 h)	50	175	166	−61	0.0	1.97
	r2	56	179	171	−173	2.0	2.01
	r3	−174	−174	−59	−59	3.2	
	r4	−173	−174	−55	−175	5.8	
	r5	−172	−172	−175	−175	9.2	
	r6	−174	−81	−65	−75	10.5	
	r7	−82	−174	−74	−65	10.5	

[a] Dihedral angles are defined as follows: φ_1 = C1−C2−C3−C4; φ_2 = C2−C3−C4−C5; ω_1 = H10−C2−O6−H7; and ω_2 = H11−C4−O8−H9 (see Figure 7 for atom numbering). [b] Relative electronic energies calculated at the MP2/cc-pVQZ//MP2/cc-pVTZ level.

The average interaction energy corresponding to the O−H···O−H interactions, $\hat{E}_{in}$, is calculated according to

$$\hat{E}_{in} = \frac{E_{in}}{N-1} \tag{6}$$

Table 4 also lists the $\hat{E}_{in}$ values obtained for the HP clusters. As can be seen, the average interaction energy depends on the size of the cluster, making necessary some knowledge on the average size of the actual HB structures to provide a realistic value. Experimental techniques present limited sensibility to cluster size,[45] and molecular dynamics simulations have been regarded as the ultimate solution for the determination of liquid structures.[44−46] According to recent simulations on liquid linear alcohols, the mean number of HBs per molecule is about 1.8,[46] corresponding to linear chains averaging 10 molecules. The same average length was obtained from WAXS measurements (sensitive only to average lengths) in linear alcohols.[49] A recent Raman study[45] also provides a good qualitative agreement with the cluster size distributions obtained using MDs.[46] The extrapolated total interaction energy for a chain of 10 molecules (obtained from the data in Table 4) is about −343 kJ/mol; hence, the average interaction energy for the autoassociation of HP is $\hat{E}_{in} \sim -38$ kJ/mol.

To complete the picture of the autoassociation of PVA, it is necessary to consider the formation of intramolecular HB-s (IHB-s) with vicinal repetitive units. The model compound 2,4-dihydroxypentane (DHP) can be analyzed to briefly discuss these IHB-s, and Figures 7g and 7h display a meso diad (m-DHP) and a racemo diad (r-DHP), respectively. In case of m-DHP the vicinal IHB is formed when the main chain adopts the tt conformation, while the tg conformation is necessary case of r-DHP (see models **7g** and **7h**). The strength of the IHB-s cannot be calculated exactly but can be estimated using different approaches.[50] The simplest one consists in the determination of the energy difference between the IHB conformation and the selected non-IHB conformation but is affected by certain conformational contribution. Table 5 presents the relative electronic energies for the most stable IHB and non-IHB conformations of both m-DHP and r-DHP. Only the seven conformers of smaller energy have been included for each compound, and the first two geometries actually correspond to IHB conformers. In case of m-DHP, the electronic energy of the most stable non-IHB conformers (m3 and m4) is about 12 kJ/mol above the reference level. The conformational change from m1 to m3 (or m4) involves the following main energetic contributions: first, the O−H···O HB is broken ($\Delta E > 0$); second, the conformation of the main chain changes from tt to gt ($\Delta E > 0$); and finally, one 1,5 C−H···O interaction stabilizes m3 (or m4) ($\Delta E < 0$). Consequently, the exact calculation of the HB energy is difficult. A convenient simplification is to assume that the two last contributions are of similar magnitude (expected range is 2−5 kJ/mol), approximately canceling out each other. Considering this approach, the strength estimated for the IHB-s in m-DHP is ∼12 kJ/mol. This estimate is in good agreement with the value of about 10−11 kJ/mol reported by Traetteberg et al. for 1,4-butanediol.[51,52] In the case of r-DHP, the IHB-s should be slightly weaker according to the slightly larger IHB distances (Table 4), but the small ΔE (3.2 kJ/mol) between the non-IHB conformer of smaller energy (r3) and the reference value indicated the occurrence of additional stabilizing effects in r3. In this case the main energetic contributions occurring when going from r1 to r3 are, first, the O−H···O HB is broken ($\Delta E > 0$), second, the conformation of the main chain changes from gt to tt ($\Delta E < 0$), and, finally, two 1,5 C−H···O interactions stabilize r3 ($\Delta E < 0$). The last two favorable contributions probably account for the small electronic difference between r1 and r3.

Regardless of the exact strength of the IHB, Table 5 clearly indicates that the formation of intermolecular HB-s is favored over IHB-s. For example, conformer m3 is stabilized by about −26 kJ/mol if it forms a dimer-like HB, but only by about −11.6 kJ/mol if it adopts the m1 conformation. The similar idea holds for the other conformers in the table. Nevertheless, it is important to realize that the formation of IHB-s increases the actual strength of the autoassociation interactions in bulk HP. The model adopted here for the autoassociation of alcohols assumes the formation of open chains averaging 10 molecules; therefore, about a 10% of free OH groups should be expected. However, in DHP (or in PVA) the OH groups not establishing intermolecular HB-s will prefer conformations allowing the formation of IHB-s. In fact, the "free" OH band is not detected in neat PVA (it is hardly distinguished in the temperature spectra of copolymers of vinyl alcohol),[23,24] while it is clearly observed in the spectra of other typical polyols like poly(vinylphenol).[19,53] In addition, the IHB-s could take part of the HB open chain structures, increasing their average lengths. As a consequence, the average interaction energy should increase to values closer to the saturation limit obtained in Table 4, $\Delta E_{in} \sim -40$ kJ/mol; anyway, the average interaction energy should be in the range $\hat{E}_{in} \sim -38$−40 kJ/mol.

The spectra calculated at the MP2/cc-pVDZ level for some of the models analyzed in the preceding paragraphs is shown in Figure 8. In the spectrum calculated for PP (7a) the C═O stretching band is located at 1808 cm^{-1}. The difference between the calculated and the experimental values can be corrected using scaling factor, usually in the range 0.95−0.96 at this level of theory.[53] In this paper we are mainly interested however in spectral

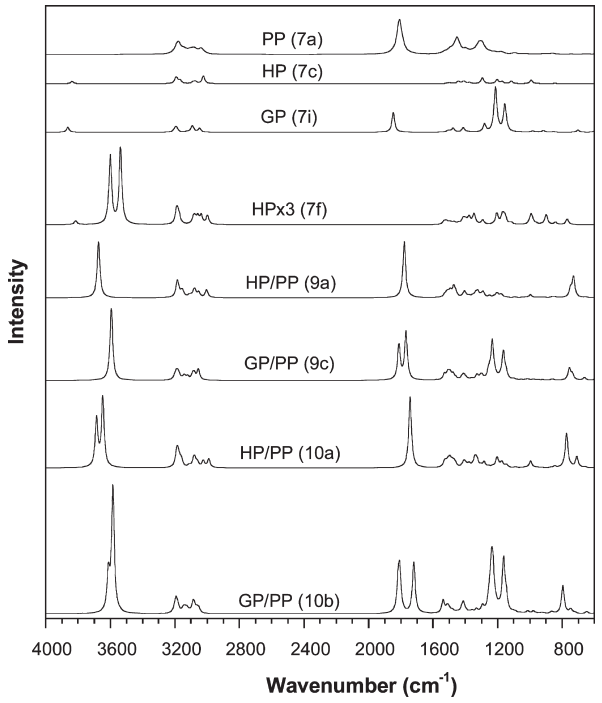

Figure 8. IR spectra for some of the model compounds and the complexes studied throughout this paper.

shifts rather than in absolute frequencies, and the unscaled frequencies will be considered. The spectrum calculated for the HP trimer (7f) is also shown. The hydroxyl stretching band of the HP cluster contains three components at about 3815, 3600, and 3537 cm^{-1}. The higher wavenumber component can be attributed to the free-like OH bond, the intermediate band to the dimer-like bond, and the lower wavenumber contribution to the multimer-like bond. Since the analysis of cooperativity with chain length does not show a noticeable dependence, multimer-like bonds in HP can be assumed to absorb at about 3540 cm^{-1}. Table 6 lists the frequencies, intensities, and interaction energies.

Figure 9 shows different complexes involving PP. Since the pyrrolidone ring is slightly bent (a fast interconversion of low activation barrier is admitted to occur between its two slightly distorted forms),[54] similar optimized geometries are actually obtained for the complexes, differenced only in whether the pyrrolidone ring bends toward the complexing partner or in the opposite direction. The geometries in which the pyrrolidone ring skews toward the second molecule are denoted in this paper without punctuation marks (i.e., 9a), and in case it skews to the opposite side a prime mark (′) is added (i.e., 9a′, see Table 6). Figures 9a and 9b present the geometries of two of the most stable complexes for the HP/PP system. As can be seen in Table 6, the interaction energy for the HP/PP complexes is about −34 kJ/mol, indicating that the intermolecular O−H···O═C interactions are weaker than the autoassociation in pure HP (average interaction energy about −40 kJ/mol). The location of the hydroxyl stretching band, considered a proper indicator of the strength of the interactions, also reflects this situation, since the calculated hydroxyl stretching band of the HP/PP system is located (on average) at higher wavenumbers (∼3660 cm^{-1} vs ∼3540 cm^{-1}, respectively). Finally, the calculated C═O stretching band of PP is red-shifted by about 36 cm^{-1}.

The results obtained for the model compound HP/PP are in good qualitative agreement with those observed in the PVA/PVP blends investigated (Figure 3, bottom part, and Figure 4). Both the model system and the blend show a noticeable blue shift for the OH stretching band. Regarding the red shift of the C═O stretching band, the difference observed between the calculated and the measured values (36 cm^{-1} vs 22 cm^{-1}) can be partially accounted for recalling that the experimental location for the "free" carbonyl band of pure PVP is actually shifted due to dipole−dipole interactions in the neat polymer.

The intermolecular interactions between the esterified residues in the g-PVA copolymers and PVP can be modeled choosing 2-glycolylpropane (GP) as HB donor (Figure 7i). GP can adopt a variety of conformations, and the geometry 7i has been used to calculate the absorption wavenumber for its free OH stretching band (∼3860 cm^{-1}; see Figure 8 and Table 6). Figures 9c and 9d show the most stable geometries obtained for the GP/PP complexes optimized at the MP2/cc-pVDZ level. Their inspection reveals that the C═O groups of the glycolyl residues adopt an antiparallel arrangement relative to the C═O groups in the pyrrolidone ring, indicating attractive dipole−dipole interactions. In fact, the optimization of the 20 initial structures attempted (containing the O−H···O═C HB) conduced in most cases to structures similar to 9c and 9d, in few cases to structures with misaligned dipoles (Figures 9e and 9f), while stable structures containing the C═O groups in parallel alignment could not be obtained. As can be seen in Table 6 and in Figure 8, the wavenumber obtained for the OH stretching band corresponding to intermolecular interactions is relatively close to the location calculated for the autoassociation of HP (3585 vs 3540 cm^{-1}), indicating O−H···O HB-s of similar strength. These calculations are hence in reasonable agreement with the behavior observed for the hydroxyl stretching band of the g-PVA/PVP system (Figure 4, upper side). The fact that the strength of the noncooperative O−H···O═C intermolecular interaction is similar to that of the cooperative O−H···O−H autoassociation suggests that the introduction of ester groups in the β carbon strengthens the HB interaction, probably through electronic effects. However, the total intermolecular interaction in the GP/PP system is about 12 kJ/mol stronger than the autoassociation of HP (52 kJ/mol vs 40 kJ/mol), indicating the occurrence of significant additional contributions to the interaction strength. We propose that most of the additional interaction energy can be attributed to dipole−dipole interactions. Notice for example that in the 9d geometry a large part of the GP molecule does not come into VDW contact with the PP molecule because the interactions established by the O−H and the C═O groups in GP define the orientation of the rest of the molecule.

Regarding the location of the C═O stretching band, the average location for the most stable complexes of the GP/PP system is about 1765 cm^{-1}, 7 cm^{-1} below the location calculated for the HP/PP system. This result is also in good agreement with the spectral shifts obtained in the polymeric systems, where the associated C═O stretching band for the g-PVA/PVP was found to occur at about 6 cm^{-1} at lower wavenumbers than in the PVA/PVP system.

As indicated before, some of the stable complexes obtained for the GP/PP system present misaligned dipoles (Figures 9e and 9f). According to Table 6, their total electronic energies are about 6−9 kJ/mol larger than those corresponding to the most stable structures; hence, these geometries are rather improbable. As can be seen in Figure 8, in these geometries the C═O groups in the pyrrolidone ring and in the glycolyl residue adopt nearly

Table 6. CP Corrected Relative Electronic Energies (ΔE), Interaction Energies (E_{in}), and C═O and O−H Stretching Band Locations and Wavenumbers for Different Compounds and Complexes

system	geometry	ΔE (kJ/mol)	E_{int} (kJ/mol)	ν_{O-H} (cm^{-1})	I_{O-H} (au)	$\nu_{C=O}$ (cm^{-1})	$I_{C=O}$ (au)
PP	7a					1808	7.16
HP	7c			3837	0.46		
HP × 3	7f			3815	0.79		
			−63.3	3600	14.05		
				3537	15.65		
GP	7i			3863	1.04		
HP/PP	9a	0.0	−34.0	3673	11.50	1779	11.54
	9a′	0.3	−33.3	3672	11.72	1778	11.80
	9b	0.1	−34.2	3649	10.53	1767	11.16
	9b′	0.3	−34.1	3630	16.13	1765	12.38
	averages		−33.9	3656	12.47	1772	11.72
GP/PP	9c	0.0	−55.5	3594	14.82	1768	9.84
	9c′	1.2	−50.7	3577	15.37	1766	9.19
	9d	0.5	−51.2	3566	17.15	1765	9.67
	9d′	0.2	−51.5	3602	14.51	1762	9.57
	averages		−52.2	3585	15.46	1765	9.57
	9e	6.9	−46.5	3595	16.47	1776	10.65
GP/PP	9e′	7.7	−46.9	3602	15.24	1775	10.75
missaligned	9f	6.3	−48.4	3578	16.74	1766	9.88
dipoles	9f′	9.0	−44.6	3574	17.10	1765	10.64
	averages		−46.6	3587	16.39	1771	10.48
HP/PP				3685	9.85		
	10a		−67.6			1742	14.62
double HB-s				3647	14.24		
GP/PP				3612	7.58		
	10b		−105.1			1719	10.49
double HB-s				3584	25.67		

perpendicular orientations; hence, dipole−dipole interactions should be strongly reduced. In fact, the average location observed for the C═O stretching band in these complexes is 1771 cm^{-1}, close to the value observed for the HP/PP system. Their (average) interaction energy (−47 kJ/mol) is smaller than that of the most stable structures, and even though the dipole−dipole contact seems lost, they also seem to establish additional contacts using the aliphatic part of the molecule (the propane chain). In addition, the OH stretching band is located at about the same wavenumber as in the most stable structures, indicating that the decrease in interaction energy does not arise from weaker hydrogen bonds. Therefore, the smaller interaction energies of these geometries seems to arise from the loose of the dipole−dipole interactions but seems to be partially compensated by additional VDW interactions.

The strength of the dipole−dipole interactions has also been estimated using an alternative approach consisting of modeling two acetone molecules with the C═O groups located at the same relative positions as in models 9c and 9d. The CP corrected interaction energy (at the MP2/cc-pVTZ level) is −15.9 kJ/mol. To estimate the contribution of the VDW interactions to this value, the complex formed by two propane molecules has been optimized constraining the distance between the terminal CH_3 groups, leading to E_{in} = −5.4 kJ/mol. Hence, the strength of the dipole−dipole interactions estimated following this approach is 10−11 kJ/mol. Assuming that the strength of the HB-s in neat HP and in the GP/PP system are similar (as suggested by the similar location calculated for the OH stretching bands), this results suggests that most of the difference in interaction energy observed between the neat alcohol and the GP/PP complex should be attributed to the dipole−dipole interactions.

Hence, molecular modeling results indicate that primary hydroxyl groups bearing β C═O (ester) groups establish strong intermolecular interactions with the C═O groups of GP (and presumably with any tertiary amide). At the MP2/cc-pVTZ level, an interaction energy of about −40 kJ/mol can be roughly attributed to the O−H···O═C HB and an additional −10 kJ/mol to the dipole−dipole interactions. In the case of HB donors in which the C═O group is located at larger distances from the OH group, the picture of the interactions might be different. For example, in the VAHB14 copolymer the C═O group is located in the γ carbon, and the spectral behavior observed for the VAHB14/PVP blends is somewhat intermediate between those of the PVA/PVP and the VAGA44/PVP systems. However, this intermediate behavior could be actually due to the small substitution degree of the copolymer, rather than to the location of the C═O group. The cases of poly(2-hydroxyethyl methacrylate) (PHEMA) and poly(2-hydroxypropyl methacrylate) (PHPMA) are completely different because the −CO−O− group in the lateral chain is reversed. For example, in the case of PHEMA the chemical structure of the lateral group is $-R-CO-O-CH_2-CH_2OH$ (R denotes the main chain). Hence, in a hypothetical antiparallel arrangement of C═O groups (like those reported here) the negatively charged oxygen located in the backbone of the lateral chains of PHEMA will be

dx.doi.org/10.1021/ma2012305 |Macromolecules 2011, 44, 7351–7363

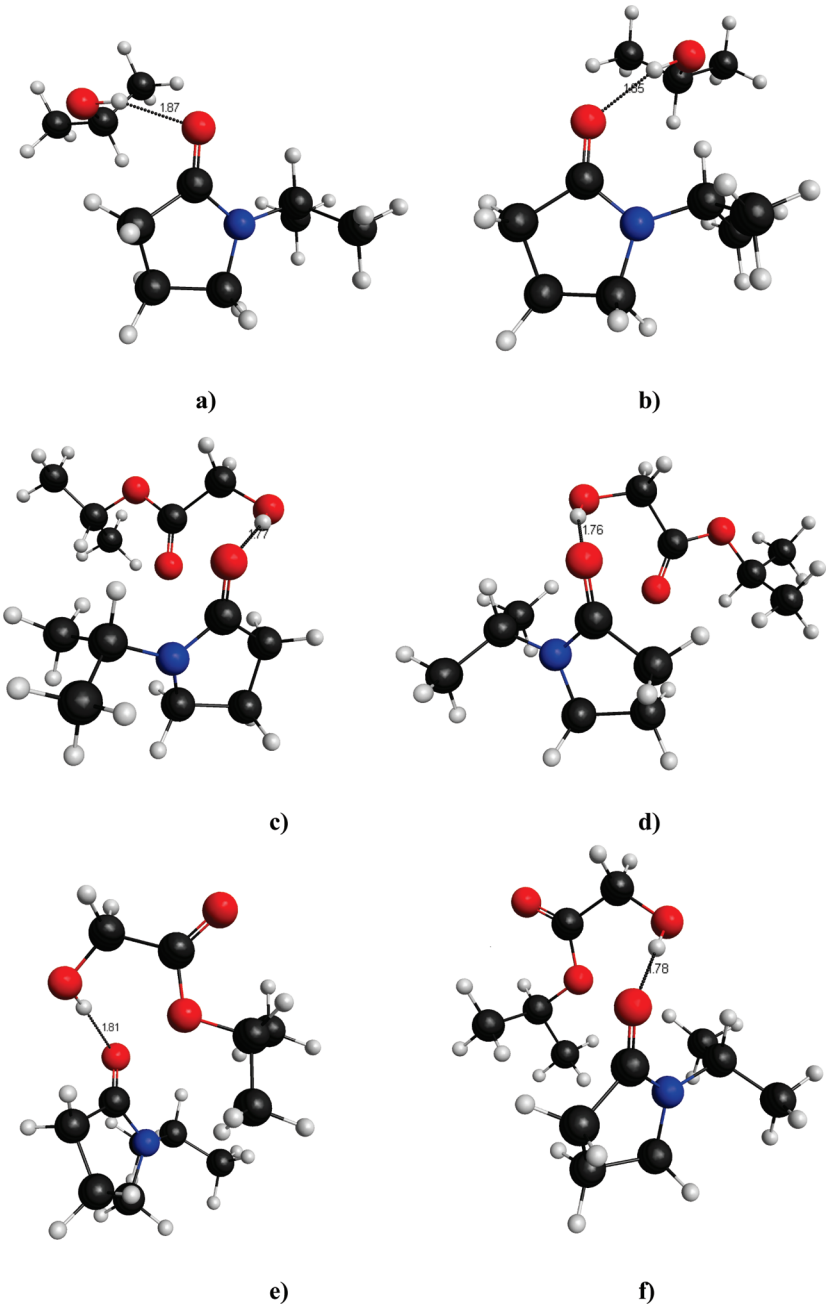

Figure 9. Equilibrium geometries for the complexes of different systems: (a, b) HP/PP system; (c, d) lower energy complexes for the GP/PP system; (e, f) higher energy complexes for the GP/PP system.

necessarily located between the interacting C═O groups, destabilizing the dipole−dipole interactions because of repulsive electrostatic interactions with the carbonyl oxygen located in the pyrrolidone ring. Actually, the PHEMA/PVP and the PHPMA/PVP blends have been investigated,[55,56] and the location found for the hydrogen-bonded C═O group of PVP in those systems is 1665 cm^{-1}, at even higher wavenumbers than in the PVA/PVP or PVPh/PVP systems, perhaps due to repulsive dipole−dipole interactions. Anyway, it is clear that the dipole−dipole interactions occurring in those systems should be completely different from those reported here.

In the g-PVA/PVP blends containing an excess of hydroxyl groups the IR spectra also show a new band located at about 1712 cm^{-1}, red-shifted by as much as 70 cm^{-1}. We have tentatively assigned this contribution to double hydrogen bonds (two hydroxyl groups act as donors and a single C═O group acts as acceptor), but such interaction is not observed in the similar PVA/PVP system and is completely unusual in the literature dealing with polymer miscibility. Hence, we have investigated the formation of double hydrogen bonds in the HP/PP system and in the GP/PP systems. Because of the large size of the systems, only a single geometry has been calculated in each case. Starting geometries were generated using the most stable geometries calculated before.

Figure 10a presents the stable geometry calculated for the HP/PP system containing a double HB. As can be seen in Table 6, the

dx.doi.org/10.1021/ma2012305 |*Macromolecules* 2011, 44, 7351–7363

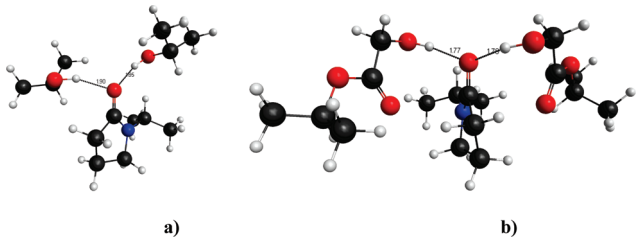

Figure 10. Equilibrium geometries for complexes containing double hydrogen bonds: (a) HP/PP system and (b) GP/PP system.

interaction energy is again smaller than the interaction energy corresponding to the autoassociation (−68 kJ/mol vs −80 kJ/mol). Considering also that these structures are more constrained than the formation of single hydrogen bonds, they should be unfavored. Figure 10b presents the stable geometry calculated for the GP/PP system containing a double HB (see Table 6). In this case, the interaction energy is again much larger than that for the autoassociation (−105 kJ/mol vs −80 kJ/mol). The calculated C═O stretching band of PP is located at 1719 cm^{-1}; hence, the red shift is 89 cm^{-1}, larger than the shift observed in the polymeric system (about 70 cm^{-1}). The difference can be accounted for considering that the experimental shift is affected by the dipole−dipole interactions in pure PVP (shifting the location observed for the "free" C═O stretching band) and also by the fact that we are not using any scaling factor (a value about 0.95 is usual at the level of theory used here). According to these results, the formation of double hydrogen bonds is energetically favored over the formation of single bonds, and the calculated shift agrees well with the measured value. Hence, molecular modeling results support the formation of double hydrogen bonds in the g-PVA/PVP system. Notice that even though all these results have been calculated for the most stable complexes, the potential energy surface of the HB complexes is usually very flat. This means that in the structure **10b** the engaged GP molecules can be rotated around the C═O bond of PP affecting only slightly to the calculated results.

Finally, the comparison of Figures 5 and 6 suggests a larger fraction of double hydrogen bonds when PVA is grafted with glycolic acid (compared to PVA grafted with lactic acid). This difference can be probably attributed to the larger esteric constraints due to the lateral methyl groups present in the lactyl residues. In addition, we guess that the origin of the blue-shifted component observed in the PVP-rich blends at ∼1692 cm^{-1} (Figure 5) might be due to repulsive dipole−dipole interactions with "free" C═O group of PVP vicinal to the actually HB C═O groups. For example, racemic diads of PVP are known to adopt preferentially the all-trans conformation,[57] resulting in sequences of C═O groups with antiparallel orientation along the PVP chain. If one of them bonds to a glycolyl residue, the neighboring "free" amide carbonyl groups will be aligned in parallel relative to the C═O group of the glycolyl residue. The analysis of these structures is however beyond the scope of this work.

■ CONCLUSIONS

Poly(vinyl alcohol) (PVA) grafted with different hydroxy acids (lactic acid (LA), glycolic acid (GA), and hydroxybutyric acid (HB)) is completely miscible with poly(vinylpyrrolidone) (PVP). The dependence of the glass transition temperature of the blends with composition obeys the Fox equation, suggesting that free volume additivity can be assumed in the blends. The analysis by FTIR of the PVA/PVP and the *g*-PVA/PVP systems indicates the occurrence of O−H···O═C hydrogen bonds between the hydroxyl groups in the donor polymer and the C═O groups of PVP. According to the analysis of the OH stretching band, HB between the C═O groups of PVP and the terminal OH groups located in the grafted residues is of similar strength to the O−H···O−H autoassociation of PVA or *g*-PVA but is stronger than the O−H···O═C interassociation with the secondary OH groups located in the vinyl alcohol segments.

In the PVA/PVP blends, two main contributions can be observed in the C═O stretching region of PVP: the "free" C═O groups absorb at about 1682 cm^{-1} and the HB C═O groups at about 1660 cm^{-1}. When PVP is blended with *g*-PVA exceeding 24% mol hydroxy acid (VAGA24, VAGA44, VALA28, and VALA45), the IR spectra show up to two HB contributions located at about 1654 and 1612 cm^{-1}. The higher wavenumber contribution (1654 cm^{-1}) occurs in the whole range of compositions and is actually attributed to the HB-s formed between the C═O groups of PVP and the terminal OH groups located in the grafted residues. The contribution at lower wavenumbers (1612 cm^{-1}) is only observed in *g*-PVA-rich blends (60/40 and 80/20 compositions) and is attributed to double HB-s (two "grafted" OH groups bonded to a single C═O group of PVP).

These findings indicate the importance of apparently subtle differences in the molecular architecture on the strength of the intermolecular interactions and therefore on polymer miscibility. In the PVA/PVP blends the HB C═O band occurs at about 1660 cm^{-1}. However, when the lateral chains of the donor polymer contain oxycarbonyl substituents (as in the case of hydroxylated polymethacrylates such as PHEMA and PHPMA), the location of the HB C═O band of PVP blue shifts to about 1665 cm^{-1}.[55,56] On the other hand, the presence of ester substituents in the lateral chains of the donor polymer (as in the case of the g-PVA/PVP blends analyzed here) red shifts the location of the HB C═O group of PVP to about 1654 cm^{-1}, and the formation of double HB-s can be also observed in donor-rich compositions. These differences can be attributed to the different strength of the carbonyl−carbonyl dipole−dipole interactions depending on the orientation in which the −CO−O− group is inserted in the lateral chain. In the case of polymer chains containing oxycarbonyl residues, the negatively charged oxygen atom in the lateral chain will impair attractive dipole−dipole interactions since it will be located between the interacting groups. In the case of polymer chains containing ester residues, the ester oxygen does not interfere in the interaction.

Molecular modeling analysis has been carried out to gain insight into the nature and the relative strength of the specific interactions. The strength of the O−H···O−H autoassociation in neat PVA has been analyzed adopting 2-hydroxypropane (HP) as model compound, resulting in a value of about −40 kJ/mol. The strength of the O−H···O═C interactions in the PVA/PVP system has been investigated using the complexes formed between HP and 2-pyrrolydonylpropane (PP), leading to a calculated value of −34 kJ/mol. Considering that in these two systems (pure HP and HP/PP) the main part of the intermolecular interactions can be attributed to the HB-s, these results agree with the shifts observed for the OH stretching band in the polymeric systems. The strength of the O−H···O═C interactions in the *g*-PVA/PVP systems has been analyzed considering the complexes formed between 2-glycolylpropane (GP) and PP, resulting in comparatively large value, −52 kJ/mol. In the

GP/PP complexes, the C═O groups located in the grafted residues and the C═O groups of PVP adopt an antiparallel arrangement, contributing to the total strength of the intermolecular interactions by about −10 to −11 kJ/mol. The dipole−dipole interactions explain the larger red shift observed for the C═O stretching band of PVP in the *g*-PVA/PVP blends and support the formation of double HB-s. The IR spectra has been calculated for the complexes modeled in this paper at the MP2/cc-pVDZ level of theory, and the calculated shifts are in good agreement with the measured shifts, considering the limitations inherent to the use of model compounds to approach a bulk polymer system.

AUTHOR INFORMATION

Corresponding Author

*Fax +34-94-601-3930; e-mail emiliano.meaurio@ehu.es (E.M.), jr.sarasua@ehu.es (J.R.S.).

ACKNOWLEDGMENT

The authors are thankful for funds from Basque Government, Department of Education, Universities and Research (GIC10/152-IT-334-10), and from MICINN (BIO2010-21542-C02-01). A.L. thanks the University of the Basque Country for a predoctoral grant.

REFERENCES

(1) Cassu, S. N.; Felisberti, M. I. *Polymer* **1997**, *38*, 3907–3911.
(2) Li, L.; Chen, N.; Wang, Q. *J. Polym. Sci.* **2010**, *48*, 1946–1954.
(3) Ohnaga, T.; Sato, T. *Polymer* **1996**, *37*, 3729–3735.
(4) Abou-Taleb, M. H. *J. Appl. Polym. Sci.* **2009**, *114*, 1202–1207.
(5) Shridhar, M. H.; Lata, P.; Viayalakshmi, R. *J. Ind. Council Chem.* **1998**, *15*, 31–33.
(6) Ping, Z. H.; Nguyen, Q. T.; Neel, J. *Makromol. Chem.* **1989**, *190*, 437–448.
(7) Seabra, A. B.; Oliveira, M. G. *Biomaterials* **2004**, *25*, 3773–3782.
(8) Hun, L.; Sixun, Z.; Zhang, B.; Tang, X. *Macromol. Chem. Phys.* **2004**, *205*, 834–842.
(9) Lejardi, A.; Etxeberria, A.; Meaurio, E.; Sarasua, J. R., submitted.
(10) Boys, S. F.; Bernardi, F. *Mol. Phys.* **1970**, *19*, 553–566.
(11) Granovsky, A. A. Firefly v. 7.1.G, http://classic.chem.msu.su/gran/firefly/index.html.
(12) Schmidt, M. W.; Baldridge, K. K.; Boatz, J. A.; Elbert, S. T.; Gordon, M. S.; Jensen, J. H.; Koseki, S.; Matsunaga, N.; Nguyen, K. A.; Su, S.; Windus, T. L.; Dupuis, M.; Montgomery, J. A. *J. Comput. Chem.* **1993**, *14*, 1347–1363.
(13) Bode, B. M.; Gordon, M. S. *J. Mol. Graphics Modell.* **1998**, *16*, 133–138.
(14) Qipeng, G.; Zhenhai, L. *J. Therm. Anal. Calorim.* **2000**, *59*, 101–120.
(15) Schneider, H. A. *J. Res. Natl. Inst. Stand. Technol.* **1997**, *102*, 229.
(16) Gordon, M.; Taylor, J. S. *J. Appl. Chem.* **1952**, *2*, 493–500.
(17) Simha, R.; Boyer, R. F. *J. Chem. Phys.* **1962**, *37*, 1003–1007.
(18) Fox, T. G. *Bull. Am. Phys. Soc.* **1965**, *1*, 123.
(19) Coleman, M. M.; Graf, J. F.; Painter, P. C. *Specific Interactions and the Miscibility of Polymer Blends*; Technomic Publishing, Inc.: Lancaster, PA, 1991.
(20) Coleman, M. M.; Painter, P. C. *Prog. Polym. Sci.* **1995**, *20*, 1–59.
(21) Purcell, K. F.; Drago, R. S. *J. Am. Chem. Soc.* **1968**, *89*, 2874.
(22) Rozenberg, M.; Loewenschuss, A.; Marcus, Y. *Phys. Chem. Chem. Phys.* **2000**, *2*, 2699–2702.
(23) Yeh, J. T.; Chen, H. Y. *J. Mater. Sci.* **2007**, *45*, 5742–5751.
(24) Antolín-Cerón, V. H.; Gómez-Salazar, S.; Soto, V.; Ávalos-Borja, M.; Nuño-Donlucas, S. M. *J. Appl. Polym. Sci.* **2008**, *108*, 1462–1472.
(25) Isasi, J. R.; Cesteros, L. C.; Katime, I. *Macromolecules* **1994**, *27*, 2200.
(26) Isasi, J. R.; Cesteros, L. C.; Katime, I. *Polymer* **1995**, *36*, 1235–1241.
(27) Hu, Y.; Motzer, H. R.; Etxeberria, A. M.; Fernandez-Berridi, M. J.; Iruin, J. J.; Painter, P. C.; Coleman, M. M. *Macromol. Chem. Phys.* **2000**, *201*, 705–714.
(28) Motzer, H. R.; Painter, P. C.; Coleman, M. M. *Macromolecules* **2001**, *34*, 8390–8393.
(29) Painter, P. C.; Pehlert, G. J.; Hu, Y.; Coleman, M. M. *Macromolecules* **1999**, *32*, 2055–2057.
(30) Max, J. J.; Chapados, C. *J. Chem. Phys.* **2007**, *126*, 154511.
(31) Kuo, S. W.; Chang, F. C. *Macromolecules* **2001**, *34*, 5224–5228.
(32) Engberts, J. B. F. N.; Famini, G. R.; Perjéssy, A.; Wilson, L. Y. *J. Phys. Org. Chem.* **1998**, *11*, 261–272.
(33) Maeda, Y.; Sakamoto, J.; Wang, S.; Mizuno, Y. *J. Phys. Chem. B* **2009**, *113*, 12456–12461.
(34) Venables, D. S.; Chiu, A.; Schmuttenmaer, C. A. *J. Chem. Phys.* **2000**, *113*, 3243–3248.
(35) Tonelli, A. E. *Polymer* **1982**, *23*, 676–680.
(36) Takahashi, O.; Kohno, Y.; Nishio, M. *Chem. Rev.* **2010**, *110*, 6049–6076.
(37) Ohno, K.; Yoshida, H.; Watanabe, H.; Fujita, T.; Matsuura, H. *J. Phys. Chem.* **1994**, *98*, 6924.
(38) Dobrowolski, J. C.; Ostrowski, S.; Kolos, R.; Jamróz, M. H. *Vib. Spectrosc.* **2008**, *48*, 82–91.
(39) Sponer, J.; Jurecka, P.; Hobza, P. *J. Am. Chem. Soc.* **2004**, *126*, 10142–10151.
(40) Cremer, D.; Kraka, E.; He, Y. *J. Mol. Struct.* **2001**, *567−8*, 275–293.
(41) Wiberg, K. B. *J. Comput. Chem.* **2004**, *25*, 1342–1346.
(42) Riley, K. E.; Hobza, P. *J. Phys. Chem. A* **2007**, *111*, 8257–8263.
(43) Kaminsky, J.; Mata, R. A.; Werner, H. J.; Jensen, F. *Mol. Phys.* **2008**, *106*, 1899–1906.
(44) Bloch, K.; Lawrence, C. P. *J. Phys. Chem. B* **2010**, *114*, 293–297.
(45) Lin, K.; Zhou, X.; Luo, Y.; Liu, S. *J. Phys. Chem. B* **2010**, *114*, 3567–3573.
(46) Lehtola, J.; Hakala, M.; Hämäläinen, K. *J. Phys. Chem. B* **2010**, *114*, 6426–6436.
(47) Ohno, K.; Shimoaka, T.; Akai, N.; Katsumoto, Y. *J. Phys. Chem. A* **2008**, *112*, 7342–7348.
(48) Aleman, C.; Casanovas, J. *J. Mol. Struct. (THEOCHEM)* **2004**, *675*, 9–17.
(49) Vahvaselkä, K. S.; Serimaa, R.; Torkkeli, M. *J. Appl. Crystallogr.* **1995**, *28*, 189–195.
(50) Buemi, G.; Zuccarello, F. *J. Mol. Struct. (THEOCHEM)* **2002**, *581*, 71.
(51) Traetteberg, M.; Hedberg, K. *J. Am. Chem. Soc.* **1994**, *116*, 1382.
(52) Lopes Lesus, A. J.; Rosado, M. T. S.; Reva, I.; Fausto, R.; Ermelinda, M.; Eusébio, S.; Redinha, J. S. *J. Phys. Chem. A* **2008**, *112*, 4669–4678.
(53) Bouteiller, Y.; Poully, J. C.; Desfrancois, C.; Grégoire, G. *J. Phys. Chem. A* **2009**, *113*, 6301–6307.
(54) Riggs, N. V. *Aust. J. Chem.* **1985**, *38*, 1585–1589.
(55) Kuo, S. W.; Shih, C. C.; Shih, J. S.; Chang, F. C. *Polym. Int.* **2004**, *53*, 218–224.
(56) Huang, C. F.; Kuo, S. W.; Lin, F. J.; Wang, C. F.; Hung, C. J.; Chang, F. C. *Polymer* **2006**, *47*, 7060–7069.
(57) Dubrovin, V. I.; Panov, V. P. *Vysokomol. Soedin., Ser. A* **1979**, *21*, 2741−2748 [*Polym. Sci., Ser. A* **1979**, *21*, 2741−2748].